Eur. Phys. J. B **16**, 455–462 (2000)

THE EUROPEAN PHYSICAL JOURNAL B

EDP Sciences

Non ergodic aging in potassium niobo-tantalate crystals

P. Doussineau[1,a], T. de Lacerda-Arôso[2], and A. Levelut[1]

[1] Laboratoire des Milieux Désordonnés et Hétérogènes[b], Université Pierre et Marie Curie, Case 86, 75252 Paris Cedex 05, France
[2] Departamento de Física, Universidade do Minho, 4709 Braga codex, Portugal

Received 17 November 1999

Abstract. Slow dynamics has been studied in various potassium niobo-tantalate crystals (KTN) by recording the complex dielectric constant after several thermal histories: isothermal evolution following controlled cooling or rapid quenching, positive or negative temperature cycles. The results reveal most of the behaviours of aging already found in lithium-potassium tantalate (KLT): effective ergodicity breaking (the asymptotic value of the dielectric constant varies as the logarithm of the cooling rate R), quasi-independence of the isothermal evolution with respect to a sojourn at lower temperature. But some differences between KTN and KLT are noticeable: coefficients of $\log|R|$ with opposite signs, role of the quenching temperature on the subsequent evolution, no overshot after a temperature jump. In order to explain the results we propose to extend the model initially developped for KLT taking into account the different nature of the low temperature phase, paraelectric for KLT and ferroelectric for KTN. In this model the variations of the dielectric constant are attributed to the slow movements of polarization domain walls hindered by static random fields. By measuring the dielectric constant during cooling and immediate heating at the same rate, an illustrative comparison is provided, showing that the evolution of the domain size is reversible in KLT and not in KTN.

PACS. 77.22.Gm Dielectric loss and relaxation – 78.30.Ly Disordered solids

1 Introduction

Aging is a very interesting aspect of slow dynamics in frustrated systems driven out of equilibrium. As it is well known a system ages if its dynamics is non stationary. Many disordered materials such as polymers [1], spin glasses [2,3], structural glasses [4] and disordered dielectrics [5] have shown physical aging. In particular Struik has observed the evolution of several polymers after having applied a stretching force on them [1]. He showed that this evolution was a function of the time that the sample had spent under that physical constraint. This was probably the first comprehensive study of aging.

More recently many experimental studies have been done below the transition temperature T_g of spin glasses (SG). They have shown time evolution on both the isothermal magnetization and alternative magnetic susceptibility depending on the thermal and magnetic history [2,3]. However, even if the system is started from different states, after different evolutions the steady temperature susceptibility curves seem to tend towards the same asymptote: apparently a single final state is reached. According to the classical definition of ergodicity, a system is ergodic if a unique equilibrium state is attained independently of the initial conditions. Therefore, SG can be said to be ergodic or, possibly, to present weak ergodicity breaking if the time needed to reach the unique equilibrium is infinite [6].

For some disordered dielectric materials, namely potassium-lithium tantalate (KLT) and strontium-calcium titanate (SCT), aging has also been seen in dielectric constant measurements at low temperatures [5,7,8]. In both, isothermal time evolution is observed in the complex susceptibility after the system had been cooled from a temperature above the glassy transition temperature T_{tr} down to the experiment temperature T_{exp}. In those dielectric materials there is a direct relationship between the cooling rate used in approaching T_{exp} and the final state reached by the system at this temperature [5]. In that case, ergodicity is broken, at least on an experimental time scale. Indeed, since the convergence towards a unique equilibrium state after some years cannot be excluded, it is cautious to say that KLT and SCT show effective ergodicity breaking.

In common with potassium-lithium tantalate (KLT), potassium niobo-tantalate (KTN) compounds are also solid solutions resulting from the substitution of some ions of the perovskite quantum paraelectric $KTaO_3$ by other ions which have or may acquire a dipolar moment. At low temperatures, the former stays in a paraelectric phase

[a] e-mail: dous@ccr.jussieu.fr
[b] Associated with the Centre National de la Recherche Scientifique (UMR 7603)

while the latter enters a disordered ferroelectric phase. This is a strong incitement to a comparative study of aging in KTN and KLT.

In the present article we report on experimental data obtained on KTN samples. We first present the characteristics of the material and some details on the experimental method. Then we give our data on aging observed on the complex dielectric constant after different thermal histories. Finally we compare our results with those obtained on KLT and we propose an explanation based on a modified domain model.

2 Experiments

2.1 The material

Potassium tantalate $KTaO_3$ is a perovskite crystal that would undergo a para-ferroelectric phase transition at 0 K if the zero point thermal fluctuations would not prevent it. Actually, its dielectric constant is nearly divergent and its optic T_{1u} mode softens as T goes to 0 K [9]: this is a quantum paraelectric or an incipient ferroelectric [10]. If in a potassium tantalate crystal some Ta^{5+} ions are randomly substituted by isoelectronic Nb^{5+} ions, the resulting mixed potassium niobo- tantalate crystal $KTa_{1-x}Nb_xO_3$ exhibits a polar phase at finite low temperatures. Alike pure niobium tantalate, a sequence of phase transitions involving the symmetry changes cubic-tetragonal-orthorhombic-rhombohedral is revealed in KTN; the last three phases are ferroelectric. The phase diagram of $KTa_{1-x}Nb_xO_3$ for low niobium concentrations ($x \leq 0.1$) has been reported [11]. It presents a multicritical point near $x = 0.02$ where the four phase changes merge into a single one. Between $x = 0.01$ and $x = 0.02$ there is only one transition, from cubic to rhombohedral symmetries (however, agreement is not general: glass-like properties are sometimes suggested [12]). Below $x = 0.01$ the transition leads to a dipolar glass phase.

2.2 The method

2.2.1 Apparatus and samples

Dielectric constant measurements were performed with a HP-4192A impedance analyzer using an oscillating field of around 10^3 V m^{-1} (except for some non linear measurements). No biasing electric field was applied during the course of experiments. The capacitance and the loss were measured at seven frequencies ranging from 1 kHz to 1 MHz. They can be easily transformed into the real and imaginary parts ε' and ε'' of the complex dielectric constant. However it is simpler to give the capacitance C' as it was measured (in pF) and to transform the loss into the same unit (C'' in pF). The values of geometrical factor which allows to transform capacitance into dielectric constant are written below for each sample. In contrast to KLT, both parts in KTN exhibit sufficient variations so that accurate measurements can be performed on them. Results on both are reported in this paper. Another difference with KLT is that C' and C'' are frequency dependent, even at the lowest temperatures.

The samples are monocrystalline, parallelepipedic shaped with cubic (100) faces. Their typical size is $1 \times 2 \times 4$ mm^3. Electrodes made of chromium thin films were deposited by a sputtering technique on the largest faces. For our samples both C' and C'' present a maximum at a temperature independent of the measuring frequency. We identify this temperature with the transition temperature $T_{\rm tr}$. The Nb concentrations of our samples are deduced from the phase diagram [11] once the transition temperature $T_{\rm tr}$ is measured. Since the maximum is unique, and $T_{\rm tr}$ is close to 36 K, we may deduce that the concentrations x are in the vicinity of the multicritical point. More precisely, we measure $T_{\rm tr} = 31$ K, $T_{\rm tr} = 35$ K and $T_{\rm tr} = 38$ K for the three samples we have investigated and we deduce $x = 0.022$, $x = 0.024$ and $x = 0.027$. The factors which allow to transform the capacitance (in pF) into the relative (dimensionless) dielectric constant are 20, 5.5 and 16, respectively.

2.2.2 Different thermal histories

All the reported experiments begin with an annealing at 55 K, about 20 K above the phase transition temperature $T_{\rm tr}$ for a few minutes. It was carefully checked that such an annealing was sufficient to completely erase the effect of anterior experiments. The lowest temperature used is $T_{\rm m} = 4.8$ K, slightly higher than the liquid helium boiling point, in such a way to have a better temperature control. Consequently, during isothermal measurements which may last 400 000 s, temperature was maintained constant within ± 0.01 K.

In the first series of experiments, the sample was cooled at a constant rate R down to the fixed temperature $T_{\rm exp}$. Then isothermal measurements were performed either at $T_{\rm exp} = 4.8$ K or at $T_{\rm exp} = 9.75$ K. Several cooling rates ranging from $R = -0.011$ K s^{-1} to $R = -0.27$ K s^{-1} were used. Once $T_{\rm exp}$ attained, the sample capacitance and loss isothermally decay.

In the second series of experiments, the sample was cooled at a constant rate R down to a quenching temperature $T_{\rm q}$ where the sample is suddenly (in less than 40 s) cooled to $T_{\rm m} = 4.8$ K. For a given cooling rate R, the temperature $T_{\rm q}$ was varied between $T_{\rm tr}$ and $T_{\rm m}$.

In the third series of experiments, the sample was cooled at a constant rate R down to a first temperature T_1 where the isothermal aging is recorded for the duration t_1. Then temperature is suddenly changed to T_2 where the evolution is followed for the duration t_2. Finally, temperature is driven back to the first one T_1 and aging is recorded again. These temperature cycles are named positive if $T_2 > T_1$ or negative if $T_2 < T_1$.

We emphasize that after a temperature change, positive or negative, of a few kelvins thermalisation of the sample is achieved in less than 60 s.

3 Results

3.1 Non linear dielectric constant

Bidault and Maglione [13] have observed for several samples a dependence of KTN dielectric constant on the biasing electric field at temperatures above $T_{\rm tr}$, only on the even powers since they studied the paraelectric centrosymmetric phase. This incited us to look for similar effects. However, we have used another method: at 100 kHz the oscillator level was varied in such a way that the electric field between the electrodes ranged from 10 $\mathrm{V\,m^{-1}}$ to 10^3 $\mathrm{V\,m^{-1}}$ in the $x = 0.024$ sample. We have observed that the complex capacitance is a function of the strength of the applied oscillating field $E_0\cos(\omega t)$. This indicates a non linear behaviour of the dielectric constant. The characteristics of these non-linearities are as follows: they are weak at low temperatures; they are also weak for $T > T_{\rm tr} \cong 35$ K; they are noticeable on the left hand side of the peak (between about 20 K and 35 K). These features are in favour of a symmetry change at $T_{\rm tr}$ into a non centrosymmetric phase, therefore ferroelectric according to the phase diagram [11]. Moreover, we have recorded the time evolution of C' for over 100 000 s at $T_{\rm m}$ for several a.c. field amplitudes between 10 $\mathrm{V\,m^{-1}}$ and 10^3 $\mathrm{V\,m^{-1}}$. Within experimental accuracy the aging part is independent of the measuring a.c. field. These two types of results allow to perform all our measurements with 10^3 $\mathrm{V\,m^{-1}}$ as long as the temperature is not too close to $T_{\rm tr}$.

3.2 Isothermal aging

Data of isothermal decays of both C' and C'' recorded at 100 kHz are shown in Figures 1 and 2 for various cooling rates R. At $T_{\rm exp} = 4.8$ K (Fig. 1), they show that the faster the cooling rate the lower the values of C' at any time (part a). This is an unusual behaviour if we refer to the behaviour of C' in KLT [5] and to that of C' and C'' in SCT [7] where the faster the cooling rate the higher the values. However the imaginary part C'' show the usual behaviour (part b). At $T_{\rm exp} = 9.75$ K (Fig. 2), if the behaviour of C'' (part b) is the same as in Figure 1, the behaviour of C' (part a) is much more complex: the initial values are larger if R is larger but the long time value is inverted; that means that the curves relative to different cooling rates cross after 100 000 s or 200 000 s.

To fit the isothermal decaying data (either C' or C'') a few empirical functions are tried: they are the sum of a constant with another function that tends towards zero as time goes to infinity. The two best fits correspond to stretched exponential $f_1(t)$ and to power law $f_2(t)$

$$f_1(t) = A + B\exp\big[-\big((t+t_0)/\tau\big)^{\gamma}\big]\big/\exp\big[-(t_0/\tau)^{\gamma}\big]$$
$$f_2(t) = A + B\big((t+t_0)/t_0\big)^{-\alpha}.$$

In both equations constant A stands for the asymptotic values C'_∞ or C''_∞ while the sum $A + B$ represents the initial values. A least square method gives fits of similar figures of merit for the two functions. However the power law function is preferred because it contains only four free parameters.

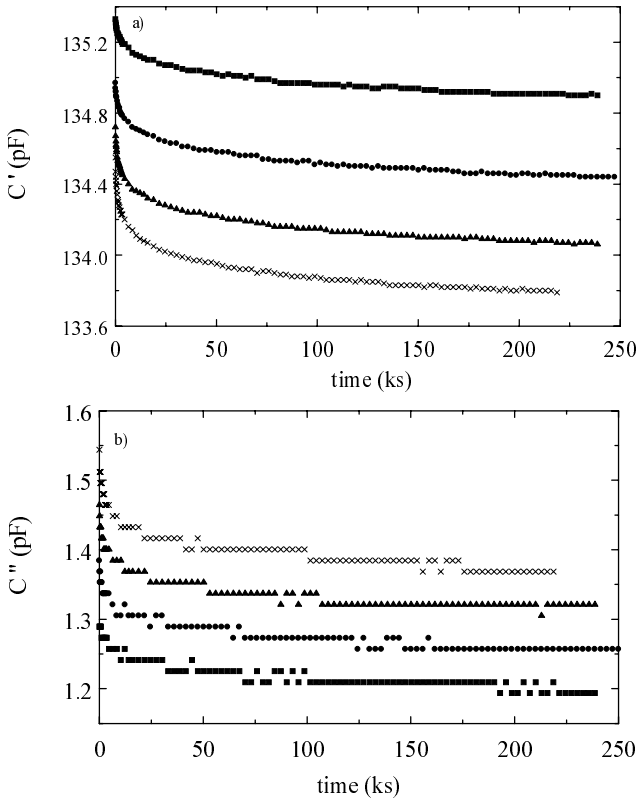

Fig. 1. Isothermal complex capacitance ($C = C' - \mathrm{i}C''$) as a function of time measured at 100 kHz in a sample of $KTa_{1-x}Nb_xO_3$ ($x = 0.027$). Data were recorded at $T_{\rm exp} = 4.8$ K after different cooling rates R: -0.011 $\mathrm{K\,s^{-1}}$ (squares), -0.022 $\mathrm{K\,s^{-1}}$ (circles), -0.044 $\mathrm{K\,s^{-1}}$ (triangles), -0.09 $\mathrm{K\,s^{-1}}$ (crosses). Part a) in-phase component; part b) out-of-phase component. Note that the order of the curves is inverted in the two parts.

In Figure 3 the asymptotic values of the real part of the capacitance in the $x = 0.027$ KTN sample is plotted as a function of $\log|R|$ for two temperatures. The plots of the extrapolated values C'_∞ show logarithmic dependences on the cooling rate with negative slopes. This last result is in contrast with what we got in KLT and SCT where the slopes are positive. The exponent α ($\alpha \leq 0.15$) of the power law is smaller than what is measured in KLT [5]. A so small value for α indicates that the trend towards the asymptotic values C'_∞ and C''_∞ is very slow and explains why the C' value after 250 ks is still larger than C'_∞.

3.3 Aging after quenching

There is a net difference between the dependence on the quenching temperature $T_{\rm q}$: in KTN the asymptote C'_∞ is a flat function of $T_{\rm q}$ just below $T_{\rm tr}$ while in KLT its variation is fast in this region [5]. For low $T_{\rm q}$, the behaviours are inverted: a flat curve for KLT in contrast to a rapid decrease for both the asymptote C'_∞ and the exponent α for KTN α These features have perhaps to be related to the unusual behaviours reported in Figures 1 and 2.

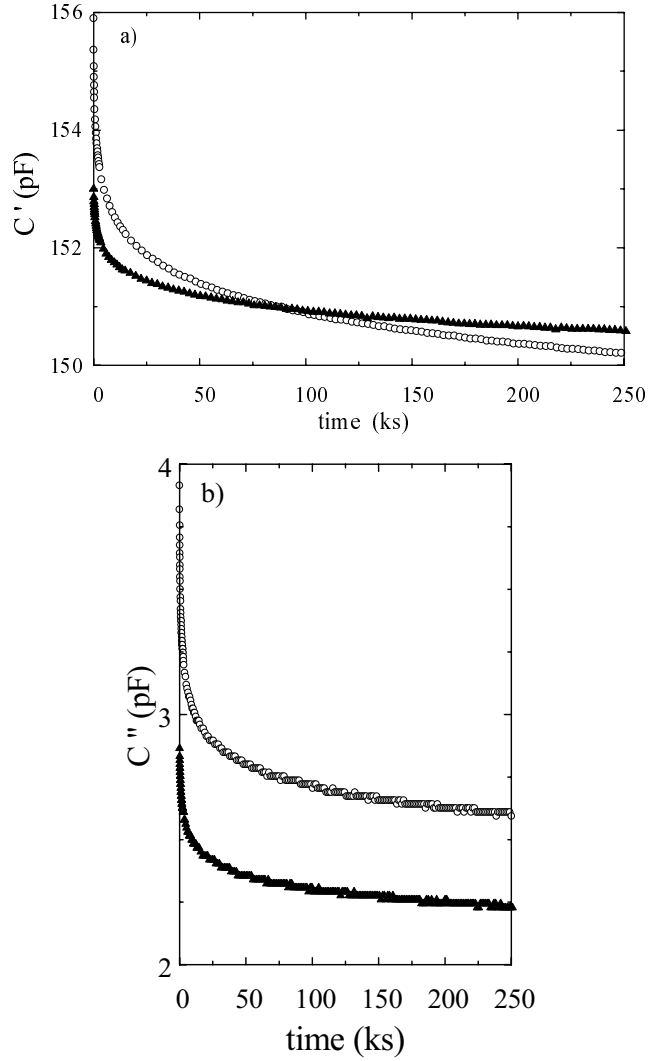

Fig. 2. Isothermal complex capacitance ($C = C' - \mathrm{i}C''$) as a function of time measured at 100 kHz in a sample of $KTa_{1-x}Nb_xO_3$ ($x = 0.027$). Data were recorded at $T_{exp} = 9.75$ K, after two cooling rates R: $-0.015\ \mathrm{K\,s^{-1}}$ (full triangles) and $-0.27\ \mathrm{K\,s^{-1}}$ (open circles).

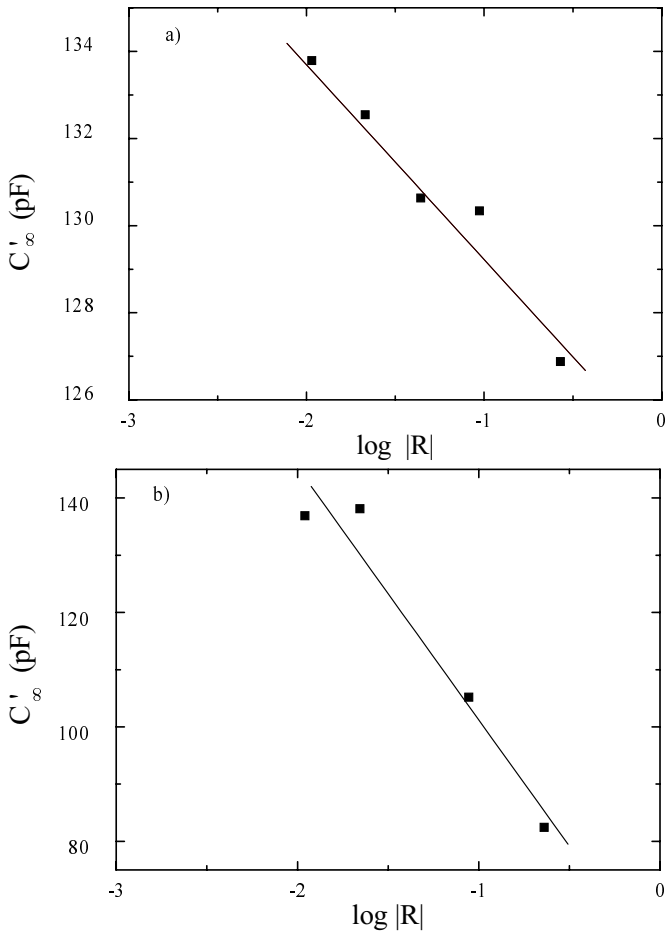

Fig. 3. Real part C'_∞ of the extrapolated (to infinite time) isothermal dielectric capacitance of the $KTa_{1-x}Nb_xO_3$ sample with $x = 0.027$ as a function of the logarithm of the cooling rate. The actual duration of these experiences varies between 250 000 s and 400 000 s. Part a) $T_{exp} = 4.8$ K; part b) $T_{exp} = 9.75$ K.

3.4 Temperature cycles

In Figure 4 the evolutions of the capacitance during a negative temperature cycle are exhibited. Since $T_1 = 8.4$ K and $T_2 = 4.8$ K are both in the ferroelectric phase, the magnitudes of C' is smaller at T_2 than at T_1. The isothermal decay is the usual manifestation of aging. The process that takes place during t_1 is interrupted by the $T_1 \rightarrow T_2$ temperature jump and another aging starts at T_2. When the temperature is changed anew to T_1 a third aging period starts. If we try to put in continuity the first and the last one of these curves we notice that they match together apart from a small positive time adjustment Δt. It looks as if the aging which started in the first part and which was nearly frozen during t_2 continues afterwards. Keeping $t_1 = 10\,000$ s, we have measured the translation t_r ($t_r = t_2 - \Delta t$) as a function of the time t_2 spent at the lowest temperature. The data are displayed in Figure 5 together with the bisector of the axes. The data points lay below this line corresponding to null translation time. The translation time Δt tends towards a constant value as the time t_2 increases.

We emphasize that the evolution immediately after a temperature jump (positive or negative) is monotonic. This is in contrast to what we have observed in KLT where the dielectric constant passes by a maximum (overshot) after a positive temperature jump [14].

For positive temperature cycles, the second period at $T_2 > T_1$ acts simply as annealing and aging is restarted in the third period. This is similar to what is seen in KLT [5].

4 Interpretation

Most of the effects (aging, ergodicity breaking, etc.) observed in KTN and reported in the previous sections are already known to also occur in KLT. In the latter, a model was proposed in order to explain the observed time dependent features [15]. Accordingly, one may wonder

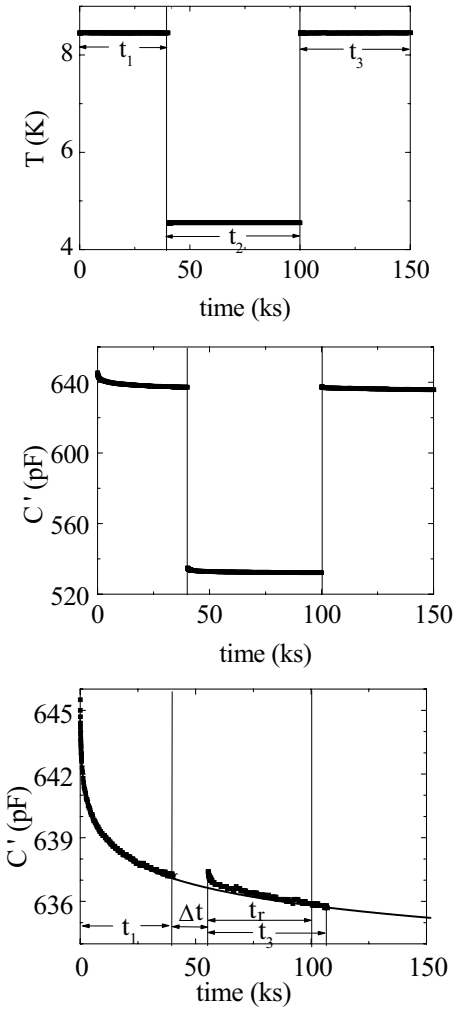

Fig. 4. Capacitance measurements of the $KTa_{1-x}Nb_xO_3$ sample with ($x = 0.024$) performed during a negative temperature cycle between temperatures T_1 and T_2. Upper part: temperature variation ($T_1 \rightarrow T_2 \rightarrow T_1$) as a function of time. Middle part: untreated capacitance measurements at T_1 and T_2. Lower part: capacitance measurements at T_1 only; the first period is drawn as measured while the last period has been translated towards the left by the time $t_r = t_2 - \Delta t$ in such a way that it is in continuation of the first one.

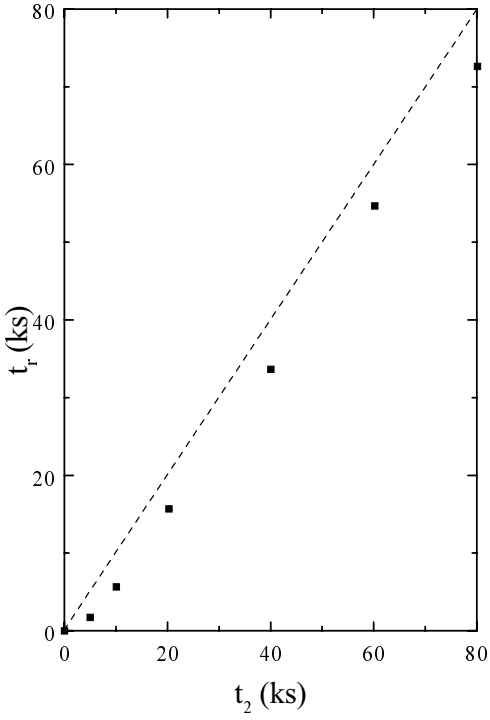

Fig. 5. Data obtained on the $KTa_{1-x}Nb_xO_3$ sample with $x = 0.024$ during a negative temperature cycle between temperatures T_1 and T_2. The translation t_r is given as a function of the duration t_2 at temperature T_2. For long t_2 the data points tend to be on a line parallel to the bisector and below it.

if the same model is also able to account for the similar (but not identical) features seen in the former. Our first step is therefore to briefly remind the main lines of this model. Indeed, there are differences in some behaviours of KTN as compared to KLT: no overshot occurring after a temperature jump, but memory effect and return to disorder observed after a temperature plateau [16]. Therefore, in the second step we discuss the modifications which can be done in the domain model in view of its application to KTN. These modifications allow to explain some of our results.

4.1 The domain model for KLT

Pure potassium tantalate is an incipient ferroelectric in which the occurrence of ferroelectric order is prevented by quantum fluctuations. If a fraction of the K^+ ions are substituted by Li^+ ions the trend towards ferroelectricity is hindered. However, when the temperature is lowered, the dielectric constant still increases, thus indicating the presence of polarization domains. Their equilibrium size is the fluctuation coherence length $\xi \propto \sqrt{\varepsilon'}$. This length varies as $T^{-1/2}$, except at very low temperatures ($T \leq 5$ K) because of zero point fluctuations. The key assumption of the model [15] is that the slowly varying contribution to the dielectric constant reflects the slow growth of the domains of polarization of the lattice, mainly due to Ta^{5+} ions. It is slow because the jump of the Ta^{5+} ions is hindered by the static random fields generated by the Li^+ ions frozen at low temperatures. More precisely, the time dependent effect is attributed to the domain walls. As time elapses, the typical domain size ρ increases at the given temperature T, tending towards $\xi(T)$, individual wall area increases as ρ^2 while the domain number decreases as ρ^{-3}. As a result, the dielectric constant must decrease with time (roughly speaking as ρ^{-1}), as we actually observe. In this scheme, the motion of the domain walls is twice: an oscillating motion forced by the radiofrequency measuring field and a slow motion towards the equilibrium size. The result is the contribution $\delta\varepsilon(\omega, t)$ which depends on both frequency and time. If the static random fields are assumed to induce energy barriers, the law of domain growth is deduced: the size ρ logarithmically increases with time. This means that the growing rate decreases when the size increases.

For $T > T_{tr}$, there are no more static random fields and consequently $\rho = \xi$.

The model explains most of the observed features provided that a domain size distribution is introduced. Three types can be distinguished: fast domains which are always in equilibrium, slow domains which are frozen below T_{tr} and intermediate domains which present slow dynamics, logarithmic dependence on the cooling rate R, effect of quenching, etc. [17]. It also includes the surprising non monotonic behaviour after a positive temperature jump (overshot). In this case, some fast domains have already reached a size close to the large equilibrium size at the low temperature T_1 and they have to slim when the temperature is suddenly increased to some temperature $T_2 > T_1$. Indeed this slimming process is very slow but a nucleation process provides a fast fragmentation. This induces an initial increase of C'. Afterwards the growth of the slow domains is dominant again and C' then decreases.

4.2 The domain model for KTN

In the temperature range where our experiments have been performed, KTN is in a ferroelectric phase in contrast to KLT which stays in a paraelectric phase. As a consequence there are two characteristic lengths in KTN. The first one is the fluctuation coherence length $\xi \propto \sqrt{\varepsilon'}$ which is maximum at the transition temperature T_{tr} and decreases from T_{tr} down to the lower temperatures. The second one is the polarization coherence length λ which would be infinite in a perfect ferroelectric in thermal equilibrium. In the paraelectric phase ($T > T_{tr}$) the two lengths coincide since the average polarization is equal to zero. In fact, in KTN the intentionally substituted Nb^{5+} ions act as static random fields [18] which hinder the domain growth. As a consequence the polarization domains may not freely grow and a very long time is needed to reach their equilibrium size.

As in KLT, we assume that the fundamental role is played by the separating walls between regions of different polarizations. For $T \geq T_{tr}$, domain growth is fast, equilibrium size is reached and ρ equals ξ. Below T_{tr}, the domain size may, in principle, grow up without limit as λ is infinite. Here lies an important difference with KLT. For $T < T_{tr}$, in KTN, upon cooling as well as upon heating the size ρ increases, more or less rapidly according to the temperature and to the size itself. This is in contrast with the behaviour in KLT where $\xi(T)$ is always a limit (or an attractor) for ρ. Of course, if T crosses T_{tr} from below, because KTN becomes paraelectric as KLT is, the domain size in KTN must slim towards $\xi(T)$.

Obviously, the preceding description is an oversimplified view. Indeed there exits a distribution of domain sizes since every domain evolve according to its own rate. Here again, there is a difference between KTN and KLT. In both cases there are very slow, nearly frozen domains, the size of which does not vary. But in KTN there are no domains able to reach the ferroelectric equilibrium size since it is infinite and their growing rate is low. All the KTN domains which are not practically frozen correspond to the intermediate domains in KLT.

As in KLT the logarithmic growth of domains in KTN explains the observed aging while the splitting into slow and fast domains is at the origin of the effective ergodicity breaking. This splitting, which depends on the cooling rate R, also explains the variation of the asymptote with R. The overshot observed in KLT and explained by the slimming of the too large domains is not seen in KTN because the domains have never to slim in the ferroelectric phase.

4.3 A pedagogical experiment

Another experiment also corroborates our view of aging. It confirms that the original domain model is well appropriate to KLT and shows that it is also convenient for KTN when modified in a quite natural manner. For this purpose the capacitance in these two materials has been measured during the same thermal history: cooling from T_{tr}, at a constant rate $R < 0$, down to $T_m = 4.8$ K, followed immediately by heating at the opposite rate. The behaviour of the relevant lengths is now to be examined.

During cooling, between instants $t = 0$ and $t = t_d$, the fluctuation coherence length in KLT increases from $\xi(T_{tr})$ up to $\xi(T_m)$ according to $\xi(T) = \xi(T_{tr})\sqrt{T_{tr}/T}$, being $T(t) = T_{tr} + Rt$. During heating, then $R > 0$, between instants t_d and $2t_d$, $\xi(T)$ decreases from $\xi(T_m)$ down to $\xi(T_{tr})$ in a symmetrical way with $T(t) = T_m + R(t - t_d)$. This is sketched in Figure 6a by the two symmetric dotted lines. The size $\rho(t)$ of a neither too fast nor too slow evolving domain is also shown in Figure 6a. During cooling, $\rho(t)$ first follows $\xi(T(t))$ up to a value which depends on R, then it continues to increase but slower than ξ. After t_d, during heating, although ξ is a decreasing function of time, $\rho(t)$ continues to grow until $\xi(t) = \rho(t)$. After that, the domain begins to slim but even slower than $\xi(T(t))$ because of its large size. Its time evolution accelerates as temperature increases and finally $\rho(t)$ reaches $\xi(T(t))$ at T_{tr}. The dashed line between t_d and $2t_d$ in Figure 6a is the symmetric of $\rho(t)$ from 0 to t_d. The difference between the full and the dashed curves is zero at t_d and at $2t_d$ and therefore it has an extremum in between. This result is also valid for ρ^{-1} and so for the dielectric constant too.

The difference between the capacitance measured at 100 kHz in $K_{1-y}Li_yTaO_3$ with $y = 0.017$ during cooling and heating $\Delta C' = C'_h - C'_c$ is displayed in Figure 7a as a function of temperature. Its value is zero at $T_m = 4.8$ K, passes through a minimum near 21 K, (nearly in the middle of T_m and $T_{tr} = 34$ K) and finally returns to zero close to T_{tr} where the domains can freely evolve because the static random fields vanish. The agreement between this result and the behaviour above predicted is very satisfying.

In KTN too, the domains can freely evolve above T_{tr} in such a way that $\xi(t) = \rho(t)$. From T_{tr} to T_m the domain size $\rho(t)$ grows slower and slower as T decreases.

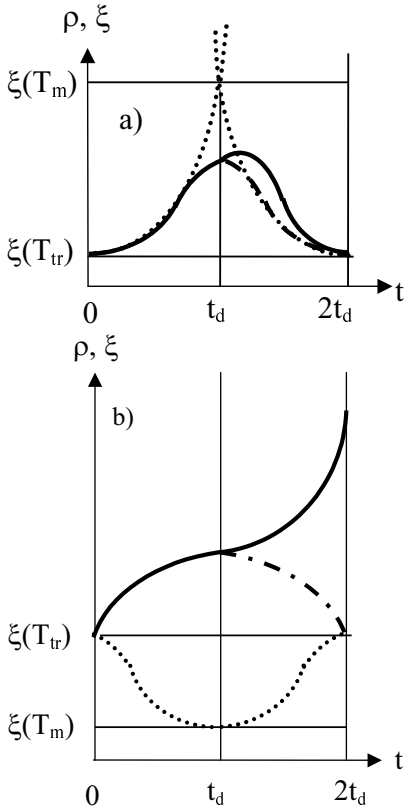

Fig. 6. Schematic representation of the evolution of the fluctuation coherence length ξ (two dotted lines) and of the size of a typical domain ρ (full line) during the following thermal history: from time 0 to time t_d, cooling from T_tr down to T_m followed immediately from time t_d to time $2t_\mathrm{d}$ by heating from T_m up to T_tr. The dashed lines represent the symmetric (during heating) of the evolution of ρ during cooling. The full lines and the dashed lines are valid for a given temperature change rate $|R|$. Part a) KLT, part b) KTN.

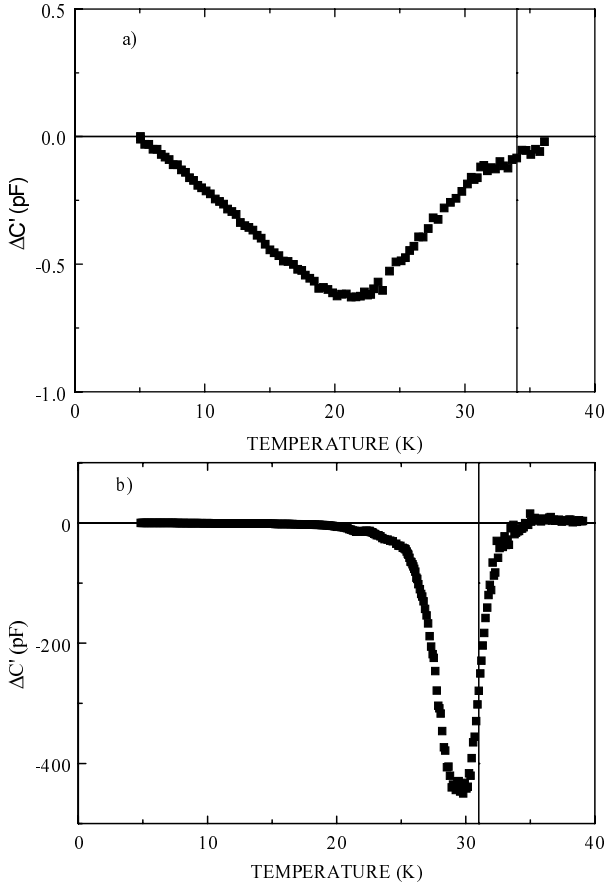

Fig. 7. Part a) difference between the capacitance of a KLT crystal with the lithium concentration $y = 0.017$, measured during heating from T_m up to T_tr and the capacitance measured at 100 KHz just before during cooling from T_tr down to T_m. The vertical line marks the transition temperature $T_\mathrm{tr} = 34$ K of the lithium dipole freezing. Part b) same as in part a) but measured at 1 kHz for the KTN crystal with the niobium concentration $x = 0.022$. The vertical line marks the para-ferroelectric transition temperature $T_\mathrm{tr} = 31$ K. Note the different capacitance scales in the two parts.

When the sense of temperature variation is inverted the polarization domain length $\rho(t)$ keeps growing now faster and faster as the temperature approaches T_tr. A schematic representation of $\rho(t)$ evolution during this thermal sequence is drawn in full line in Figure 6b, while the dashed line is the symmetric of $\rho(t)$ from 0 to t_d. The difference between the full and the dashed curves is null at t_d and increases during the whole heating till $2t_\mathrm{d}$. The same kind of monotonic behaviour occurs in ρ^{-1}, *i.e.* in the dielectric constant.

The difference between the capacitance of KTN with $x = 0.022$ measured at 1 kHz during cooling and heating $\Delta C' = C'_\mathrm{h} - C'_\mathrm{c}$ is displayed in Figure 7b as a function of temperature. Starting from zero at $T_\mathrm{m} = 4.8$ K it monotonically decreases as expected from the domain size evolution. Just below $T_\mathrm{tr} = 31$ K it reaches a minimum and rapidly goes to zero as the sample enters its paraelectric phase. Patently there is a good agreement between this result and the behaviour just predicted, though a small deviation (≈ 1.5 K) of the experimental minima from the expected one at T_tr is observed; this shift is probably due to the transition hysteresis.

Figure 7 clearly puts in evidence the different behaviours of these two materials. The minimum at intermediate temperature (near 21 K) of the curve shown in Figure 7a demonstrates that the domain size first increases and then decreases in KLT. On the contrary the curve of Figure 7b does not present such a minimum at intermediate temperature. This shows that the domain size always increases in the ferroelectric phase of KTN. This is in agreement with the absence of overshot after a temperature jump in KTN.

5 Conclusion

KLT and KTN crystals are materials obtained by substitution in the same lattice of different ions acting as static random fields. KLT remains paraelectric while KTN enters a ferroelectric phase at low temperatures. However they share common properties.

Our dielectric measurements show that they both present effective ergodicity breaking with a logarithmic variation with respect to the cooling rate (Sect. 3.2). Quenching at different temperatures generates changes of the asymptotic value (Sect. 3.3). The responses to temperature cycles are similar: a positive cycle induces a simple annealing while a negative cycle is somewhat paradoxical since the actually observed relaxation during the sojourn at low temperature may be quasi totally cancelled by a time translation (Sect. 3.4).

However, they present noticeable differences. The logarithmic dependences of ergodicity breaking on the cooling rate have opposite signs. The consequences of quenching are seen near $T_{\rm tr}$ for KLT and at low temperatures for KTN. During cycles, KLT shows a surprising overshot which is absent in KTN.

A model which attributes the time dependent effects to the slow motion of the walls of polarization fluctuations, hindered by static random fields, was successfully proposed for KLT. In this model the domain sizes are geometrically characterized by a single length but a distribution of the sizes has to be introduced. One may wonder whether this model, modified in order to contain the ferroelectric nature of KTN, would describe the effects observed in this material. The main difference between these two materials is that the size of the domains is limited in KLT (finite fluctuation coherence length ξ) while it can grow infinitely in KTN (infinite polarization coherence length λ). We have qualitatively taken into account the existence of these two lengths and tested the consequences. In a back and forth experiment (Sect. 4.3), the difference between KLT and KTN predicted by the modified model is clearly observed. This agreement gives us some confidence in our modifications.

However, in spite of this first improvement, several remarkable features are not yet explained (effect of quenching, memory, return to disorder, for instance). The model has still to be improved, may be by a better characterization of the domains with more than one length, or by a more precise geometrical description of their surface, and also by the role of the pinning centers which slow down any motion in the crystals.

We thank J.P. Bouchaud for numerous and fruitful discussions and S. Ziolkiewicz for the crystal growth.

References

1. L.C.E. Struik, *Physical Aging in Amorphous Polymers and Other Materials* (Elsevier Scientific Publishing Company, 1978).
2. É. Vincent, J. Hammann, M. Ocio, L. Cugliandolo, in *Sitges Conference on Glassy Systems*, edited by M. Rubi (Springer, Berlin, 1997).
3. L. Lundgren, P. Svedlinh, P. Nordblad, O. Beckman, Phys. Rev. Lett. **51**, 911 (1983).
4. R.L. Leheny, S.R. Nagel, Phys. Rev. B **57**, 5154 (1998).
5. F. Alberici, P. Doussineau, A. Levelut, J. Phys. I France **7**, 329 (1997).
6. J.P. Bouchaud, J. Phys. I France **2**, 1705 (1992).
7. F. Alberici, M.R. Chaves, P. Doussineau, T. de Lacerda-Arôso, A. Levelut, J. Phys. Cond. Matt. **9**, 6447 (1997).
8. P. Doussineau, A. Levelut, S. Ziolkiewicz, Europhys. Lett. **33**, 391 (1996).
9. R.L. Prater, L.L. Chase, L.A. Boatner, Phys. Rev. B **23**, 221 (1981); H. Chou, S.M. Shapiro, K.B. Lyons, J. Kjems, D. Rytz, Phys. Rev. B **41**, 7231 (1990).
10. D. Rytz, A. Châtelain, U.T. Höchli, Phys. Rev. B **27**, 6830 (1983).
11. M.D. Fontana, E. Bouziane, G.E. Kugel, J. Phys. Cond. Matt. **2**, 8681 (1990).
12. D. Sommer, W. Kleemann, D. Rytz, Ferroelectrics **106**, 137 (1990).
13. O. Bidault, M. Maglione, J. Phys. I France **7**, 543 (1997).
14. F. Alberici, P. Doussineau, A. Levelut, Europhys. Lett. **39**, 329 (1997).
15. F. Alberici-Kious, J.P. Bouchaud, L. Cugliandolo, P. Doussineau, A. Levelut, Phys. Rev. Lett. **81**, 4987 (1998).
16. P. Doussineau, T. de Lacerda-Arôso, A. Levelut, Europhys. Lett. **46**, 401 (1999).
17. F. Alberici-Kious, J.P. Bouchaud, L. Cugliandolo, P. Doussineau, A. Levelut (unpublished).
18. W. Kleemann, Int. J. Mod. Phys. B **7**, 2469 (1993).